

Title: Particle surface area, ultrafine particle number concentration, and cardiovascular hospitalizations

Authors: Shao Lin^{a,b*}, Ian Ryan^a, Sanchita Paul^c, Xinlei Deng^a, Wangjian Zhang^d, Gan Luo^e, Guanghui Dong^f, Fangqun Yu^f

Affiliations:

^a Department of Environmental Health Sciences, University at Albany, State University of New York, Rensselaer, NY, USA

^b Department of Epidemiology and Biostatistics, University at Albany, State University of New York, Rensselaer, NY, USA

^c Department of Environmental & Sustainable Engineering, University at Albany, State University of New York, Albany, NY, USA

^d Department of Preventive Medicine, School of Public Health, Sun Yat-sen University, Guangzhou, China

^e Atmospheric Sciences Research Center, University at Albany, State University of New York, Albany, NY, USA

^f School of Public Health, Sun Yat-sen University, Guangzhou, China

***Corresponding author:**

Shao Lin, MD, PhD, Professor

Department of Environmental Health Sciences

Associate Director of Global Health Research

School of Public Health

University at Albany, State University of New York

One University Place, Rm 212d

Rensselaer, NY 12144

Office phone: (518) 402-1685; Fax: (518) 402-0329; E-mail: slin@albany.edu

Abstract

While the human health impacts of larger particulate matter, such as PM_{10} and $PM_{2.5}$, have been studied extensively, research regarding ultrafine particles (UFPs or $PM_{0.1}$) and particle surface area is lacking. This case-crossover study assessed the associations between exposure to particle surface area concentration (PSC) and UFP particle number concentration (UFPnc) and hospital admissions for cardiovascular diseases (CVDs) in New York State (NYS), 2013-2018. We used a time-stratified case-crossover design to compare the PSC and UFPnc levels between hospitalization days and control days (similar days without admissions) for each CVD case. We utilized NYS hospital discharge data to identify all CVD cases who resided in NYS. We used UFP simulation data from GEOS-Chem, a state-of-the-art chemical transport model, to define PSC and UFPnc. Using a multi-pollutant model and conditional logistic regression, we assessed CVD risk per inter-quartile change of PSC and UFPnc after controlling for meteorological factors, co-pollutants, and time-varying variables. Our results indicate an immediate and robust positive association between PSC and overall CVDs (lag0–lag0-1: 1.0%) and a delayed, lasting effect between UFPnc and CVDs (lag0-3–lag0-6: 0.4%). Exposure to larger PSC was associated with immediate increases in stroke, hypertension, and ischemic heart diseases (0.7%, 0.8%, 0.8%, respectively). The adverse effects of PSC on CVDs were highest among youngest children (0-4 years old), in fall and winter, and during cold temperature days (2.0%, 1.4%, 1.3%, 1.5%, respectively) compared to those on other days. We found an immediate, positive effect of PSC on overall CVDs and a delayed, lasting impact of UFPnc. PSC was a more sensitive indicator than UFPnc. The PSC-related effects were higher among certain CVD subtypes, in the youngest children, in certain seasons, and during cold days. Further studies are needed to validate our findings and evaluate the long-term effects.

Keywords: ultrafine particles, particle surface area, air pollution exposure, cardiovascular admission, lag effect, vulnerable population, seasonality

Introduction

While relatively large particulate matter, such as PM₁₀ (those smaller than 10 µm) and PM_{2.5} (those smaller than 2.5 µm), have been associated with adverse health outcomes in many prior studies (Schraufnagel 2020; Li et al. 2017), few know that ultrafine particles (UFPs) may threaten human health even more than larger particles. Classically, PM has been classified by size, an important factor in determining its health impacts. Airborne particulates smaller than 100 nm or ≤0.1 µm in diameter are called UFPs or PM_{0.1} (these two terms are used interchangeably in this paper). Sources of UFPs include engine combustion, products of cooking, indoor heating and wood burning, new particle formation and growth, and more recently, products generated through nanotechnology. Studies have shown that exposure to ambient UFPs has detrimental effects on respiratory and cardiovascular systems (Schraufnagel 2020). Compared to larger particles, UFPs are of a more public health concern due to their 1) uniquely small size, which allows them to move into the lung interstitium and periphery easily, 2) large surface area to mass ratio, allowing them to attach to trace metals/chemicals, and 3) ability to penetrate the alveoli and translocate to other organs via systemic circulation quickly (Schraufnagel 2020; Chen et al. 2020; HEI 2013).

There is mounting evidence from prior studies that show the adverse health effects of PM_{2.5} on cardiovascular diseases (CVDs). However, fewer studies have examined the CVD effects of UFPs (Schraufnagel 2020; Brook et al. 2010; Du et al. 2016). In addition, among the few UFP studies, UFP number concentration (UFPnc) was found to be associated with multiple CVDs, such as ischemic heart diseases (IHDs), stroke, hypertension, myocardial infarction (MI), and heart failure, but not found in PM_{2.5} or PM₁₀ (Li et al. 2017; Chen et al. 2020; Andersen et al. 2010; Downward et al. 2018). However, despite the rapid growth of published studies on UFPs over the past decade, the evidence regarding the associations between UFP exposure and cardiovascular effects remains inconclusive due to the paucity of epidemiologic studies in this area exposure misclassification, and lack of standard metrics.

Most previous studies assessed the effect of UFPs on respiratory diseases rather than on CVD, although CVD is the leading cause of death in the US, leading to 659,000 deaths (1 in 4) each year (CDC 2018). In addition, heart disease costs the US approximately \$363 billion per year (Aparicio et al. 2021), and CVD is the top primary cause for hospital admissions in New York State (NYS). In addition, there are currently no regular UFP monitoring sites in the US or

other countries. As a result, almost all published papers in this area used UFP measurement data from one or very few monitoring sites, usually located in urban areas. Since UFPs have high spatial variability, the limited number of special monitoring sites introduces significant exposure misclassification problems and limited generalizability for studies utilizing them.

Furthermore, fine particle metrics other than particle number concentration have been rarely used to assess their health effects in prior research. For instance, Chen et al. (2020) found that particle surface area concentration (PSC) was associated with a higher risk of MI than UFPnc, and PSC may be a more sensitive and biologically relevant metric. Finally, previous studies have not considered the interaction of meteorological and seasonal factors with UFPs on CVD, although these factors are considered important effect modifiers (Sioutas et al. 2005).

This study helps fill the knowledge gaps described above by assessing the association between PSC and UFPnc on hospital admissions for overall CVDs and several major CVD subtypes in NYS using simulated data generated by the innovative GEOS-Chem-model (17 * 17 miles grids). We also estimated the effects of PSC on CVD across lag days, socio-demographics, seasons, and meteorological factors.

Method

Study design and health outcomes

We used a time-stratified case-crossover design where days of admission are defined as case days while identical weekdays in the same calendar month are defined as control days (Zhang et al. 2018; Rich et al. 2019). Since each case is compared with him/herself on control days, all personal confounders such as gender, age, family history of heart disease, and genetic variations are automatically controlled.

We obtained CVD-related hospital admissions data from the New York Statewide Planning and Research Cooperative System (SPARCS), a legislatively mandated database covering over 95% of hospital records in NYS (Zhang et al. 2018). We defined CVDs using principal diagnosis, the International Classification of Diseases (ICD) 9: 390-459, and ICD-10: I00-I99. In addition, we included the following major CVD subtypes for stratified analysis: 1) cerebrovascular diseases (ICD-9: 430-438, ICD-10: I60-I69), 2) hypertensive diseases (ICD-9: 401-405, ICD-10: I10-I16), 3) IHDs (ICD-9: 410-414 and ICD-10: I20-I25), 4) acute rheumatic fevers (ICD-9: 390-392 and ICD-10: I00-I02), 5) chronic rheumatic heart diseases (ICD-9: 393-398 and ICD-10: I05-I09), and

6) diseases of pulmonary circulation (ICD-9: 415-417 and ICD-10: I26-I28). All hospital admissions were geocoded to the street level and assigned to one of the GEOS-Chem simulation grids to be matched with the exposure variables.

PSC and UFP Simulation Model and Data

Due to the absence of a statewide network of PSC and UFP monitors, this study relied on particle size distribution simulations generated by GEOS-Chem-APM, a state-of-the-art global chemical transport model equipped with a size-resolved advanced particle microphysics (APM) module (Yu and Luo 2009). The GEOS-Chem model is a global 3-D model of atmospheric composition (Bey et al. 2001) and is continuously being improved (Luo et al. 2020; Holmes et al. 2019; Keller et al. 2014; Murray et al. 2012; Pye and Seinfeld 2010; Evans and Jacob 2005; Martin et al. 2003). The APM model has the following relevant features to accurately simulate particle size distributions: (1) 40 bins to represent secondary particles with high size resolution for the size range important for the growth of nucleated particles to CCN sizes (Yu and Luo 2009); (2) a state-of-the-art Ternary Ion mediated Nucleation (TIMN) mechanism (Yu et al. 2018) and temperature-dependent organics-mediated nucleation (Yu et al. 2017); (3) explicit kinetic condensation of both H_2SO_4 and low volatile organic gases onto particles (Yu 2011); and (4) explicit resolution of the coating of secondary species on primary particles. GEOS-Chem-APM has been used in several studies, and modeling results have been evaluated against a large set of land-, ship-, aircraft-, and satellite-based measurements (Yu and Luo 2009; Yu et al. 2017; Yu 2011; Yu et al. 2010; Yu et al. 2012; Yu et al. 2015; Yu et al. 2016; Yu et al. 2018; Luo and Yu 2011; Ma et al. 2012; Ma et al. 2014; Williamson et al. 2019).

In the present study, we ran GEOS-Chem-APM over a nested domain in the northeastern US with a $0.3125^\circ \times 0.25^\circ$ horizontal resolution. PSC and UFPnc were calculated based on simulated particle size distribution (see Fig. 1 in Results for an example).

Statistical analysis

We used conditional logistic regression to evaluate the association between the rate of overall cardiovascular diseases with the PSC and UFPnc. Specifically, we regressed the case day/control day status against these two indicators while controlling for ambient temperature, relative humidity, $\text{PM}_{2.5}$, O_3 , NH_3 , and time-varying variables, including holidays, season, and

long-time trend. Other air pollutants, such as NO₂ or SO₂, were not controlled in the model because they are highly correlated with UFPs (correlation coefficients >75%). We also conducted several stratified analyses for PSC by disease subtype, lags (0-6 days individually and cumulatively), season, and multiple sociodemographic characteristics, including age, ethnicity, and race. The excess risk (ER%) per each interquartile range (IQR) increase was calculated as $(\exp(\beta \cdot \text{IQR}) - 1) \cdot 100\%$, where β was the regression coefficient. All analysis was conducted using R 4.0.3.

Results

Particles in the atmosphere have different sizes, and particles in different sizes are dominated by different particle numbers, surface areas, and mass concentrations. The size distributions of particles in NYS are explicitly simulated using the GEOS-Chem-APM model described earlier. Figure 1 gives an example of normalized particle number, surface area, and mass size distributions at Queen College in New York City. Figure 1. describes the fractions of number, surface area, and mass in the different size ranges of particles (<0.01, 0.01-0.1, 0.1-0.5, 0.5-2.5, and 2.5-10 μm). UFPs (<0.1 μm) account for 87% of particle number concentration, 21% of PSC, and 6% of particle mass concentrations.

The associations between each IQR increase in PSC or UFPnc, and the ER for overall CVDs by cumulative and individual lag days are presented in Table 1. Overall, we found that the corresponding risks of PSC and UFPnc on overall CVDs were higher on cumulative lag days. For example, the immediate highest risk occurred for surface area on lag 0-1 (ER = 1.0%, 95% confidence interval (95% CI) = 0.7%, 1.3%) (Table 1). For UFPnc, on the other hand, the delayed highest risks were observed from lag 0-3 days to lag 0-6 days (ERs range = 0.3%-0.4%). For individual lags, the higher risks for PSC were found on lag 0-1 days, but the highest ER of UFPnc was observed on 2 days later (ER = 0.3%, 95% CI = 0.2%, 0.5%).

We compared six CVD subtypes in relations to PSC and UFPnc, which were significantly associated with cerebrovascular (stroke), hypertensive disease, and IHDs, but not with acute rheumatic fever, chronic rheumatic heart disease, and disease of pulmonary circulation on individual lag days (Table 2). In general, surface area was immediately associated with elevated risk of stroke (ER on lag 0 = 0.7%, 95% CI = 0.1%, 1.3%), hypertensive diseases (ERs range = 0.5%-0.8% for lag 0, 1, and 4 days), and IHDs (ER on lag 0 = 0.8%, 95% CI = 0.2%, 1.4%). In addition, UFPnc was statistically associated with elevated and lasting risks of hypertensive

diseases (ER on lag 2 = 0.5%, 95% CI = 0.2%, 0.8%) and IHDs (ER range = 0.4%-0.5% for lag 0, 1, 2, and 3 days).

In Figure 2, the ERs associated with each IQR increase in surface area (PSC) with the CVDs by socio-demographical characteristics on lag 0 days (the strongest lag association) were described. Generally, the associations of PSC and CVDs among different demographical groups were not statistically significant (P for interaction >0.05). However, we did observe that older adults (aged ≥ 65) were more susceptible to higher levels of PSC (ER = 1.1%, 95% CI = 0.8%, 1.3%). Interestingly, we found that very young children (<5 years) were at the highest risk (ER = 2.0%, 95% CI = 0.4%, 3.7%). Compared to their counterparts, males (ER = 1.1%, 95% CI = 0.8%, 1.4%), non-black individuals (ER = 1.2%, 95% CI = 0.9%, 1.4%), and non-Hispanic individuals, (ER = 1.1%, 95% CI = 0.9%, 1.4%) had higher risks.

Table 3 shows the ERs of PSC-CVD associations for different seasons per IQR increase in exposure. The interaction effects were statistically significant for lag 0, 1, 3, and 6 days (P for interaction <0.05). Statistically significant elevated ERs were observed for all seasons on lag 0 day. However, fall (ER of fall on lag 0 = 1.4%, 95% CI = 1.0%, 1.9%, and on lag 1 = 0.9%, 95% CI = 0.5%, 1.3%), and winter (ER of winter on lag 0 = 1.3%, 95% CI = 1.0%, 1.7%, and on lag 1 = 1.0%, 95% CI = 0.7%, 1.4%) had significant higher risks compared to spring and summer.

The interaction effects between temperature or relative humidity and PSC on CVDs were presented in Table 4. The interaction effects were constantly significant for temperature and relative humidity for most lag days (P for interaction <0.05). Compared with temperature $>90^{\text{th}}$, we found that surface area had a higher risk on CVDs when the temperature was $<90^{\text{th}}$ (ER range = 0.2%-1.5%). Similarly, the CVD risks of PSC were higher when the relative humidity was $<90^{\text{th}}$ (ER range = 0.3%-0.6%).

Discussion

Effects of PSC or UFPnc on CVDs by lag days

Our study found an immediate and strongest positive association between PSC and overall CVDs on the day of exposure and one day after. We also found a delayed adverse effect of UFP on CVD, which lasted for a week after exposure (0-3 lag days – 0-6 days). Consistent with our findings, a previous study conducted by Brook et al. (2010) stated that exposure to UFP for a few hours to weeks could trigger CVD-related morbidity and mortality in an updated

Scientific Statement from the American Heart Association (AHA). The AHA workgroup indicated that overall evidence supports a causal relationship between UFP exposure and CVD morbidity and mortality (Brook et al. 2010). In addition, Abroms et al. (2017) reported that exposure to ambient fine particulate matter increased emergency department visits for multiple cardiorespiratory outcomes during 0-2 lag days after exposure in Georgia, US. Chen et al. (2020) found that exposure to UFPs (size ranged from 10–100 nm), PSC, and particle length concentration were associated with increased risks of nonfatal MI in the first 6–12 h in Augsburg, Germany during 2005– 2015. In addition, $PM_{0.1}$ exposure was associated with an increased incidence of heart failure, acute MI, ischemic and thrombotic stroke, increased blood pressure, and worse microvascular even after controlling for $PM_{2.5}$ and NO_2 (Andersen et al. 2010). However, similar effects were not found for exposure to $PM_{2.5}$ and PM_{10} (Pieters et al. 2015; Olsen et al. 2014).

Another interesting finding from this study is that cumulative lag days may be a more endpoint-sensitive indicator representing longer time or cumulative exposure. In contrast, individual lag days demonstrate the short-term or independent effect of each day's exposure. Our findings may highlight the importance of using both single and cumulative lag days to demonstrate the short-/longer-term effects of UFP and identify the days with the highest effect for clinical facility (beds and care) preparation or public health preparedness. Unfortunately, no studies used both lag indicators to compare to our findings.

It is biologically plausible that exposure to UFP may trigger the onset of CVD in the short term, as demonstrated by multiple studies. The potential biological mechanisms include that UFP exposure may activate neural reflexes in the respiratory tract, provoke imbalance of the autonomic nervous system, and then initiate cardiac arrhythmias or MI (Brook et al. 2010). Several panel studies have also reported the associations between UFP and decreased heart rate variability within hours (Breitner et al. 2019; Rich et al. 2012) or even minutes (Petters et al. 2015) of increased exposure. In addition, short-term exposure to UFPs may cause systemic oxidative stress and inflammation, leading to impaired vascular function and thrombosis (Brook et al. 2010). A panel study of cardiac patients in Rochester, New York, observed positive associations between UFP exposure in the previous 12 hours and increased levels of fibrinogen (Croft et al. 2017).

Comparing particle surface area with UFP number concentration on CVD

Our study also found that PSC was a more sensitive indicator (with consistently higher excess CVD risks across all cumulative lag days) than UFPnc. Although UFPs accounted for 87% of UFPnc and 21% of PSC in our study, the broad range of PSC for all particles may increase the sensitivity to identify the health risks than UFPnc in our study. Consistently, Chen et al. (2020) also found that the effects of PSC and particle length concentration (PLC) were stronger and more precise than the UFPnc and remained similar after adjustment for PM or gaseous pollutants. A prior study in Augsburg, also in line with our findings, found stronger positive associations of inflammatory biomarkers in the blood with PSC and PLC than for UFPnc (Rückerl et al. 2016). Additionally, Hennig et al. (2018) reported that UFPnc (50–500 nm) and lung-deposited PSC were positively associated with overall and cardiovascular mortality in Germany.

Several toxicological studies also suggested that PSC might be the most biologically relevant and effective dose metric for acute nanoparticle toxicology in the lung (Sager et al. 2009; Schmid and Stoeger 2017). This may be explained because the particle surface is where components of UFP interact directly with bodily fluids and tissue (Schmid and Stoeger 2017). Greater PSC may increase the surface reactivity and thus the oxidative stress and pro-inflammatory effects (Hussain et al. 2009). Furthermore, Henning et al. (2018) stated that PSC distributions could be directly linked to emission sources and thus may be used for planning potential public health interventions. In other words, compared to particle mass and number, PSC could be used as an alternative metric that constitutes an integrated marker of reactive particle surface and deposition efficiency, which likely serves as a better indicator of understanding the biological mechanisms by which the inhalation of particles leads to health outcomes.

PSC/UFPnc – CVD associations by CVD subtype groups and SES

Our study found that exposure to large PSC was associated with immediate adverse effects (same day of exposure and one day after) in hospital admissions due to stroke, hypertension, and IHD. UFP's effect on IHD also occurred immediately but lasted three days after the exposure. In line with our findings, Abrams et al. (2017) reported that oxidative potential dithiothreitol exposure was associated with ED visits for multiple cardiorespiratory outcomes, including IHD, on the same day to two days after exposure in Atlanta, Georgia, US. In

addition, Karottki et al. (2015) found that outdoor UFPnc exposure was associated with adverse effects of microvascular function; and exposure to out-/in-door PM_{2.5} and bio-aerosols were associated with markers of inflammation and lung cell integrity. Furthermore, an in-home survey in near-highway and urban background neighborhoods in and near Boston (MA, USA) found that time activity adjusted annual average UFPnc exposures were associated with stroke, IHD, and hypertension after controlling for BMI (Li et al. 2017).

We did not find significant differences in the PSC-CVD associations by different strata of various sociodemographic (SES) variables. One interesting finding is that young children aged 0-4 years old showed the highest CVD risk per each IQR change of PSC. We could not find any studies that evaluated the disparities of PSC-CVD associations by SES. Children are usually more vulnerable to the health effects of air pollution, and these effects may begin in utero and produce lifelong consequences (Schraufnagel et al. 2019). As CVD is quite rare among young children, the highest CVD risk we found among young children demands further investigation.

UFP-CVD associations by seasonality and temperature

We found a significant seasonal difference in PSC-CVD relationships, i.e., the adverse effects of PSC on CVDs were approximately two-fold in the fall and winter as those in the spring or summer season. Consistently, we also found that the PSC-CVD associations were stronger on the days with lower temperature and lower humidity than hot days with high humidity. Previous studies found that when cold weather or temperature increases, UFP and other gaseous pollutant emissions can increase, matching our findings (Mathis et al. 2005). Although UFPnc near busy roads may mainly depend on emissions patterns, the diurnal or seasonal temperature cycle can also strongly modify the UFPnc and their distributions (Kuhn et al. 2005; Charron and Harrison 2003). Lower ambient temperatures favor the formation of higher numbers of the smallest particles (< 50 nm) and favor the higher rates of new particle formation and slower atmospheric dispersion, which explains why UFP numbers or PSC are usually higher in the winter than in the summer (Sioutas et al. 2005). Interestingly, Herner et al. (2006) stated that lower temperatures near the ground at night might contribute to the formation of stable atmospheric layers that trap primary pollutants near their emissions source; and this effect can thus dominate UFP concentrations in regions that are not heavily influenced by photochemistry (Herner et al. 2005). Therefore, UFP concentration, composition, and volatility exhibit significant seasonal variability

due to high spatial variability, indoor sources, variable infiltration of UFPs from various outside sources, and meteorologic conditions (Sioutas et al. 2005).

Potential mechanisms of UFP and PSC on CVD

There is sufficient reason to believe that the health effects of UFPs or $PM_{0.1}$ are greater than with larger particles because they are present in larger numbers, have a greater combined surface area, and adsorb larger concentrations of toxic air pollutants (oxidant gases, organic compounds, transition metals) per unit mass (Sioutas et al. 2005). After entering the body through the lungs, UFPs quickly translocate to all organs. Due to their small size, UFPs have unique distribution characteristics in the respiratory tree and may alter cellular function in ways that circumvent normal signaling pathways (Li et al. 2016). Additionally, UFPs can penetrate intracellularly and potentially cause DNA damage.

Another potential mechanism by which UFPs cause adverse health outcomes is lung inflammation and its subsequent spread of inflammatory mediators to distal organs. UFPs may cause systemic inflammation, endothelial dysfunction, and coagulation changes through which individuals may further develop IHD or hypertension (Schraufnagel 2020). These findings were also supported by the elevated multiple biomarkers among these patients, including C-reactive protein (CRP), circulating polymorphonuclear leukocytes, platelets, fibrinogen, plasma viscosity, and other markers after UFP exposure. Fine particles also promote endothelial dysfunction, vascular inflammation, and atherosclerosis. Increasingly, literature reports that $PM_{0.1}$ plays a major role in essentially all of these factors (Olsen et al. 2014; Hildebrandt et al. 2009). Most studies show a far greater effect for UFPs than larger particles. Furthermore, UFPs that enter alveoli can be retained in surfactant, thus sidestepping the mucociliary escalator clearance mechanisms (Möller et al. 2008). The retention half-lives of titanium dioxide particles in animal lungs are 170 days for 250-nm particles and 500 days for 20-nm particles, indicating that smaller particles cause more persistent inflammation than larger ones (Oberdorster et al. 1994).

Study strengths and limitations

To our knowledge, this is one of the few studies that have significantly improved UFP exposure assessment by using high-resolution air pollution simulation data generated by GEOS-Chem, a previously validated, state-of-the-art chemical transport model. Compared to the

relatively limited number of EPA PM_{2.5} monitors in NYS, this study utilized 286 simulation points spread out evenly over NYS at a 17 x 17-mile resolution. This unique exposure assessment models for all ambient pollutants controlled for many environmental factors, including meteorological conditions, all major exposure sources (including traffic roads, power plants, residential, agriculture, biomass burning, biogenic, ships, aviation, and others), and chemical reactions occurring in the atmosphere. Contrast to most prior UFP studies that utilized one or a few PM monitors, our unique exposure assessment can be applied to larger areas, and significantly reduced exposure misclassification bias present in previous studies. In addition to UFPnc, we also evaluated the impacts of PSC on CVD, which helped us compare and identify the most sensitive exposure metrics. Furthermore, this may be the largest study evaluating the effects of UFPs and PSC on CVD in the US as we have evaluated approximately 2 million CVD hospital admission records overall and several major CVD subtypes in NYS, one of the largest states in the US. Another advantage is our use of objective SPARCS health data to reduce reporting bias, a common limitation encountered by studies based on survey data. Finally, we used a multi-pollutant model to control for all co-pollutants in the analyses, which is a major strength compared to many prior studies that used single pollutant models.

On the other hand, several potential limitations should be considered. The first concern is how accurate the high-resolution air pollution simulations are. While GEOS-Chem has been validated around the globe by several previous studies as described in a previous session (PSC and UFP Simulation Model and Data), detailed measurements in NYS are very limited and need further validation. To this end, we have performed sensitivity analysis by using the available UFP monitoring data in two small urban areas (Queens and Rochester sites) to link with the CVD hospitalization data in the same regions. We found a similar range of excess risks (0.3%-0.7%) of overall CVD admissions and immediate effect per IQR increase of UFP in this sensitivity analysis as we originally found in our statewide study. We also found that cardiac arrhythmias, stroke, and IHD increased in the sensitivity analysis. However, the risks of stroke and IHD were not statistically significant due to the small sample sizes. Another limitation is that we only included CVD hospital admission cases, representing the most severe patients but missing the less severe cases. Therefore, the generalizability of this study may be limited. However, stroke, IHD, and most cardiovascular diseases require immediate and urgent medical attention. Therefore, it may be appropriate to use emergency department visits for these health

outcomes. In addition, our result that the youngest group (0-4 years old) showed the highest CVD risk associated with PSC is very interesting because CVDs are usually higher among adults or seniors. We evaluated the CVD subtypes among young children and found that the most common CVDs among 0-4 years old children are polyarteritis nodosa, followed by arrhythmia, congestive heart failure, and chronic pulmonary heart disease. These uncommon CVDs occurring in young children deserve further research. Finally, confounding effects are an important concern. Nevertheless, the case-crossover design has automatically controlled some inherited factors, such as age, gender, race, ethnicity, family history of CVD or other diseases, and lifestyle choices (smoking or alcohol drinking). We also controlled for all possible co-pollutants (which have correlation coefficients <0.70 with UFPs), temperature, relative humidity, and time-varying variables (weekday or weekend, holidays, season, long-term trend) in the model. However, we could not adjust for some residual confounders, such as activity patterns and indoor UFP exposure.

This study provides a useful tool for environmental scientists or epidemiologists to predict UFPnc and PSC at a much finer resolution throughout NYS than ever before. As there are currently very few UFP monitors statewide and no UFP monitor sites in rural areas, our GEOS-Chem model would significantly improve the current exposure assessment in UFP and other criteria pollutants. Our study also compared two particle metrics and their relationship with CVDs, contributing to new scientific knowledge. Furthermore, physicians and public health agencies should be aware of the transient and lasting effects of UFPs on CVDs, which could be used to prevent and intervene in those severe cases.

Conclusion

Our study found an immediate and strong positive association between PSC and overall CVDs, but a delayed, lasting effect of UFPnc on CVD. PSC was a more sensitive indicator than UFPnc. Exposure to large PSC was associated with an immediately increased risk of hospital admissions for a stroke, hypertension, and IHD. The adverse effects of PSC on CVDs were highest among youngest children (0-4 years old), fall and winter seasons, and during cold temperature days. Further studies are needed to validate our findings and evaluate the long-term effects of PSC and UFPs on CVDs and other health outcomes.

Acknowledgment and Funding source

This work was supported by Grant #86080, funded by New York State Energy Research and Development Authority (NYSERDA). We also thank the NYSDOH for providing the comprehensive health data (data sharing protocol number: 1509-01 A).

Disclaimer

This publication was produced from raw data purchased from or provided by the NYSDOH. However, the conclusions derived and views expressed herein are those of the author(s) and do not reflect the conclusions or views of NYSDOH. NYSDOH, its employees, officers, and agents make no representation, warranty, or guarantee regarding the accuracy, completeness, currency, or suitability of the information provided here.

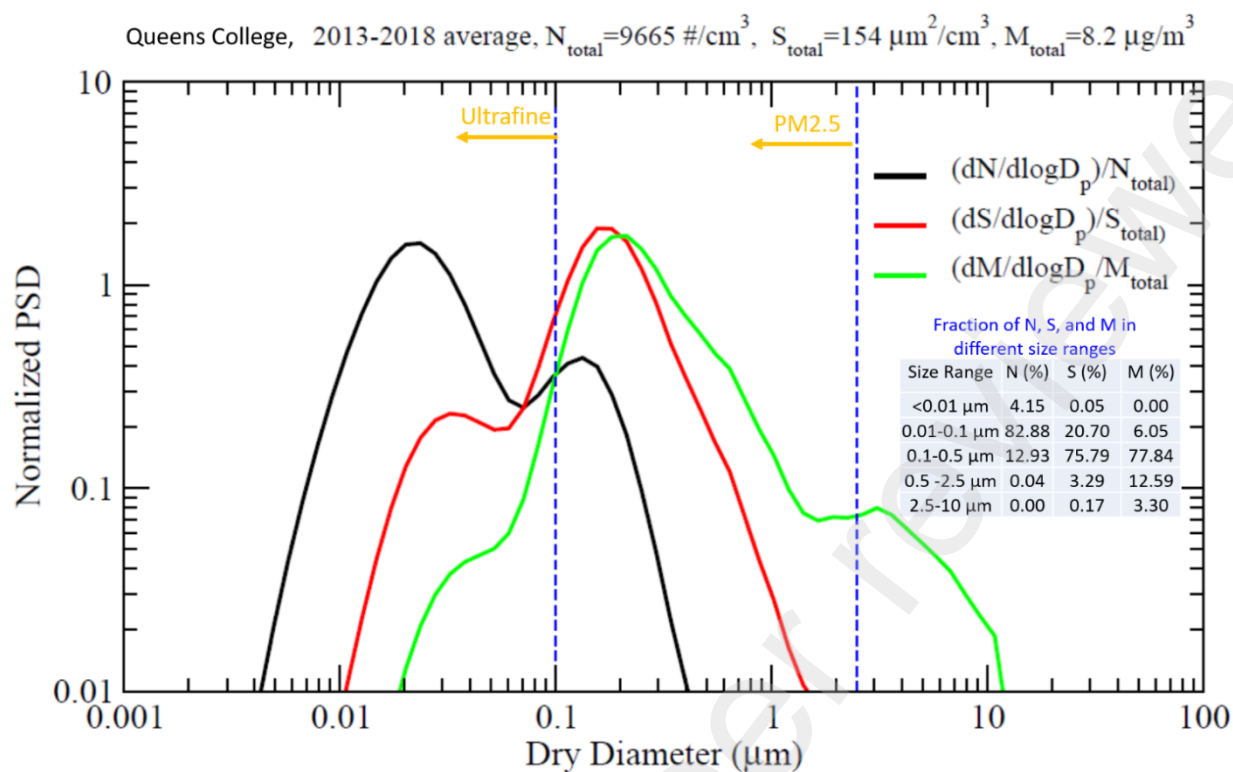


Figure 1. 2013-2018 mean normalized particle size distributions (PSD) in term of number (N, in \#/cm^3), surface area (S, in $\text{\mu m}^2/\text{cm}^3$), and mass (M, in \mu g/m^3) concentrations in an urban site (Queen College, New York City). The total N, S, and M are 9665 \#/cm^3 , $154 \text{ \mu m}^2/\text{cm}^3$, and 8.2 \mu g/m^3 , respectively. The fractions of N, S, and M in the different size ranges (<0.01, 0.01-0.1, 0.1-0.5, 0.5-2.5, and 2.5-10 μm) are given in the inserted table. UFPs (<0.1 μm) account for 87% of particle number concentration, 21% of particle surface area, and 6% of particle mass concentrations.

Table 1. Association between each IQR increase in particle surface area or number concentrations of ultrafine particles and the excess risk (%) for hospital admissions due to cardiovascular diseases.

| | Case(N) | Cumulative lags | | | Individual lags | | |
|--------------------|-----------|-----------------|--------|-----------------|-----------------|-------|-------------------|
| | | Lag | IQR | Excess Risk (%) | Lag | IQR | Excess Risk (%) |
| Surface area | 1,769,972 | 0 | 207.7 | 1.0 (0.8, 1.2) | 0 | 207.7 | 1.0 (0.8, 1.2) |
| | 1,769,049 | 0-1 | 188.8 | 1.0 (0.7, 1.3) | 1 | 207.6 | 0.5 (0.3, 0.8) |
| | 1,767,937 | 0-2 | 168.8 | 0.8 (0.5, 1.1) | 2 | 207.6 | 0.0 (-0.2, 0.2) |
| | 1,766,771 | 0-3 | 154.6 | 0.6 (0.3, 0.9) | 3 | 208.5 | -0.1 (-0.4, 0.1) |
| | 1,765,579 | 0-4 | 146.2 | 0.5 (0.2, 0.8) | 4 | 208.4 | -0.0 (-0.3, 0.2) |
| | 1,764,665 | 0-5 | 139.4 | 0.4 (0.0, 0.7) | 5 | 208.3 | -0.3 (-0.5, -0.0) |
| | 1,763,787 | 0-6 | 134 | 0.3 (0.0, 0.7) | 6 | 208.2 | 0.0 (-0.2, 0.2) |
| Ultrafine Particle | 1,769,972 | 0 | 1990 | 0.0 (-0.1, 0.1) | 0 | 1990 | 0.0 (-0.1, 0.1) |
| | 1,769,049 | 0-1 | 1835 | 0.1 (-0.0, 0.3) | 1 | 1990 | 0.2 (0.1, 0.3) |
| | 1,767,937 | 0-2 | 1706.7 | 0.3 (0.1, 0.5) | 2 | 1990 | 0.3 (0.2, 0.5) |
| | 1,766,771 | 0-3 | 1621.8 | 0.4 (0.2, 0.6) | 3 | 1990 | 0.2 (0.1, 0.4) |
| | 1,765,579 | 0-4 | 1561 | 0.4 (0.2, 0.6) | 4 | 2000 | 0.1 (-0.1, 0.2) |
| | 1,764,665 | 0-5 | 1516.5 | 0.4 (0.2, 0.6) | 5 | 2000 | 0.0 (-0.1, 0.2) |
| | 1,763,787 | 0-6 | 1480 | 0.4 (0.2, 0.7) | 6 | 2000 | 0.0 (-0.1, 0.2) |

Table 2. Excess risk (%) associated with each IQR increase in particle surface area or number concentrations of ultrafine particles by subtypes of CVD admissions in NYS

| Lag | Cerebrovascular | Hypertensive Disease | Ischemic heart Disease | Acute Rheumatic Fever | Chronic Rheumatic Heart Disease | Diseases of Pulmonary Circulation |
|--------------------|-------------------|----------------------|------------------------|-----------------------|---------------------------------|-----------------------------------|
| Surface area | | | | | | |
| 0 | 0.7 (0.1, 1.3) | 0.8 (0.3, 1.3) | 0.8 (0.2, 1.4) | -14.2 (-25.9, -0.6) | -0.5 (-6.7, 6.1) | 0.8 (-0.6, 2.1) |
| 1 | 0.4 (-0.2, 1.1) | 0.7 (0.2, 1.2) | 0.5 (-0.1, 1.1) | -8.7 (-20.6, 5.1) | 0.5 (-5.6, 6.9) | 0.9 (-0.5, 2.3) |
| 2 | 0.3 (-0.4, 0.9) | 0.2 (-0.3, 0.7) | -0.1 (-0.8, 0.5) | 6.3 (-6.5, 21.0) | 0.7 (-5.4, 7.3) | -0.3 (-1.7, 1.1) |
| 3 | -0.5 (-1.1, 0.2) | 0.1 (-0.4, 0.6) | -0.4 (-1.0, 0.2) | 2.0 (-10.9, 16.6) | 0.0 (-6.2, 6.7) | -0.4 (-1.8, 1.0) |
| 4 | -0.1 (-0.7, 0.6) | 0.5 (0.1, 1.0) | -0.7 (-1.3, -0.1) | -3.1 (-15.4, 10.9) | 3.7 (-2.8, 10.5) | -0.5 (-1.9, 0.9) |
| 5 | -0.5 (-1.1, 0.2) | -0.0(-0.5, 0.5) | -0.3 (-0.9, 0.3) | 6.4 (-7.8, 22.8) | 4.1 (-2.5, 11.0) | -0.3 (-1.6, 1.1) |
| 6 | -0.8 (-1.5, -0.2) | 0.4 (-0.0, 0.9) | 0.3 (-0.4, 0.9) | 2.6 (-10.9, 18.2) | -0.2 (-6.5, 6.5) | 0.1 (-1.2, 1.5) |
| Ultrafine Particle | | | | | | |
| 0 | 0.3 (-0.1, 0.7) | -0.3 (-0.5, 0) | 0.4 (0.0, 0.8) | -4.6 (-12.4, 4.0) | -1.2 (-4.9, 2.6) | 0.0 (-0.8, 0.8) |
| 1 | 0.3 (-0.0, 0.7) | 0.1 (-0.2, 0.3) | 0.4 (0.1, 0.8) | -2.4 (-9.9, 5.8) | -0.5 (-4.3, 3.5) | 0.2 (-0.6, 1.0) |
| 2 | -0.0 (-0.4, 0.3) | 0.5 (0.2, 0.8) | 0.5 (0.1, 0.8) | -5.0 (-12.4, 2.9) | 1.9 (-2.1, 6.0) | 1.5 (0.6, 2.3) |
| 3 | 0.2 (-0.2, 0.6) | 0.3 (-0.0, 0.6) | 0.4 (0.0, 0.8) | -2.6 (-10.2, 5.8) | 0.2 (-3.6, 4.2) | -0.4 (-1.2, 0.4) |
| 4 | 0.3 (-0.1, 0.7) | 0.1 (-0.2, 0.4) | -0.1 (-0.4, 0.3) | -1.9 (-10.0, 6.9) | 3.0 (-0.8, 7.1) | -1.4 (-2.2, -0.6) |
| 5 | 0.0 (-0.4, 0.4) | 0.0 (-0.3, 0.3) | -0.3 (-0.7, 0.1) | -5.5 (-13.2, 2.9) | -2.0 (-5.9, 1.9) | 0.3 (-0.5, 1.1) |
| 6 | 0.3 (-0.1, 0.7) | -0.1(-0.4, 0.2) | -0.1 (-0.5, 0.3) | -0.9 (-8.5, 7.4) | 0.1 (-3.7, 4.0) | -0.4 (-1.2, 0.4) |

Table 3. Excess risk (%) of overall cardiovascular admissions associated with each IQR increase in particle surface area by season, NYS

| Lag | Case | IQR | Excess risk (%) | | | | P value (seasonal difference) |
|-----|-----------|-------|-------------------|------------------|------------------|-------------------|-------------------------------------|
| | | | Spring | Summer | Fall | Winter | |
| 0 | 1,769,972 | 207.7 | 0.8 (0.4, 1.1) | 0.6 (0.2, 0.9) | 1.4 (1.0, 1.9) | 1.3 (1.0, 1.7) | P<0.001 |
| 1 | 1,769,049 | 207.6 | 0.1 (-0.3, 0.5) | 0.2 (-0.2, 0.6) | 0.9 (0.5, 1.3) | 1.0 (0.7, 1.4) | P<0.001 |
| 2 | 1,767,937 | 207.6 | -0.0 (-0.4, 0.4) | 0.0 (-0.4, 0.4) | 0.2 (-0.2, 0.6) | -0.1 (-0.5, 0.3) | 0.731 |
| 3 | 1,766,771 | 208.5 | -0.1 (-0.5, 0.3) | 0.1 (-0.3, 0.5) | 0.3 (-0.1, 0.7) | -0.6 (-1.0, -0.3) | 0.003 |
| 4 | 1,765,579 | 208.4 | -0.1 (-0.5, 0.3) | -0.0 (-0.4, 0.4) | 0.1 (-0.3, 0.5) | -0.1 (-0.5, 0.3) | 0.937 |
| 5 | 1,764,665 | 208.3 | -0.5 (-0.9, -0.1) | -0.1 (-0.5, 0.3) | -0.0 (-0.4, 0.4) | -0.4 (-0.8, -0.0) | 0.235 |
| 6 | 1,763,787 | 208.2 | -0.2 (-0.6, 0.2) | 0.4 (-0.0, 0.8) | 0.3 (-0.1, 0.7) | -0.4 (-0.7, 0.0) | 0.015 |

449
450
451
452
453
454
455
456
457
458
459
460
461
462

Table 4. Excess risk (%) of cardiovascular admissions associated with each IQR increase in particle surface area by temperature and relative humidity (RH)

| Lag | IQR (total) | Case (total) | Temp<90th | Temp>90th | RH<90th | RH>90th |
|-----|----------------|-----------------|-------------------|-------------------|-------------------|-------------------|
| 0 | 207.7 | 1,769,972 | 1.5 (1.3, 1.8)* | 0.3 (0.0, 0.6) | 0.6 (0.4, 0.8)* | 0.2 (-0.1, 0.5) |
| 1 | 207.6 | 1,769,049 | 0.8 (0.6, 1.1)* | 0.1 (-0.2, 0.4) | 0.6 (0.4, 0.8) | 0.3 (0.1, 0.6) |
| 2 | 207.6 | 1,767,937 | 0.2 (0.0, 0.5)* | -0.4 (-0.7, -0.1) | 0.3 (0.1, 0.5)* | -0.3 (-0.5, -0.0) |
| 3 | 208.5 | 1,766,771 | 0.1 (-0.2, 0.3)* | -0.6 (-0.9, -0.3) | -0.0 (-0.2, 0.2)* | -0.3 (-0.6, -0.1) |
| 4 | 208.4 | 1,765,579 | 0.1 (-0.2, 0.3)* | -0.4 (-0.7, -0.1) | 0.0 (-0.2, 0.2)* | -0.3 (-0.6, -0.1) |
| 5 | 208.3 | 1,764,665 | -0.1 (-0.3, 0.1)* | -0.8 (-1.1, -0.5) | -0.1 (-0.3, 0.1)* | -0.4 (-0.7, -0.2) |
| 6 | 208.2 | 1,763,787 | -0.1 (-0.3, 0.2) | -0.2 (-0.5, 0.1) | 0.1 (-0.1, 0.3) | 0.2 (-0.1, 0.4) |

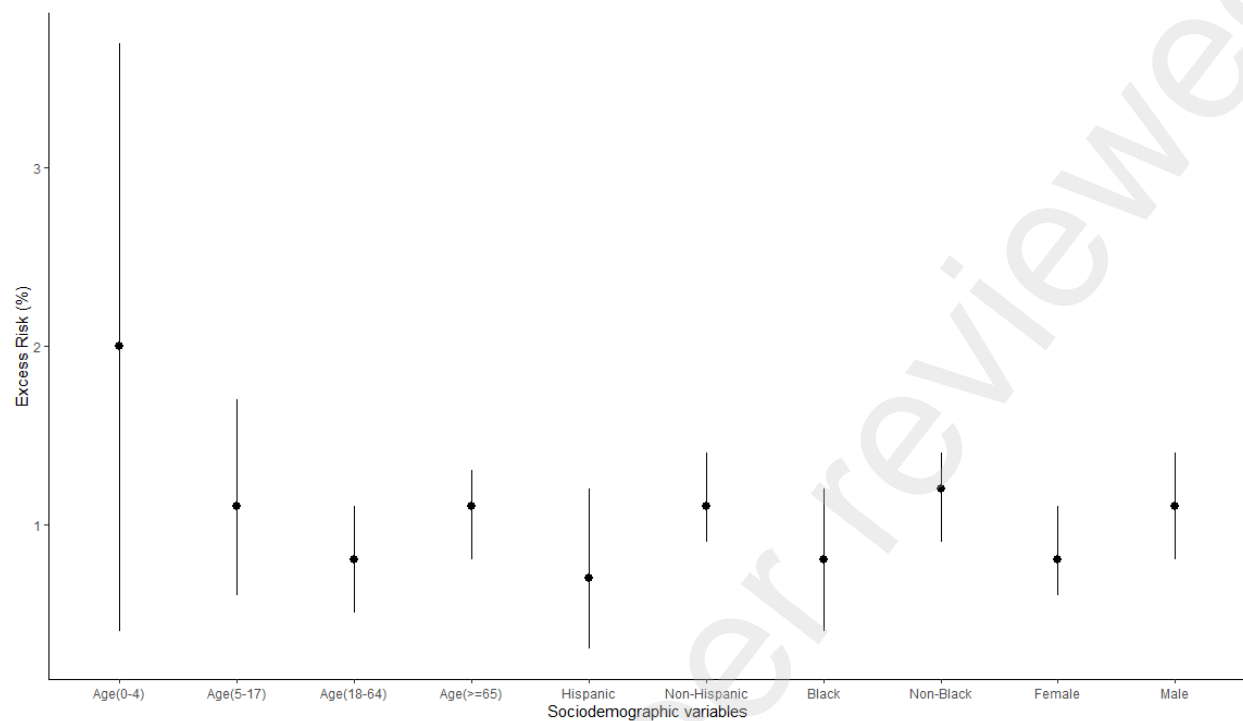


Figure 2. Association of particle surface area with overall cardiovascular hospitalization by social demographical variables

References

- Schraufnagel, D. E., 2020. The Health Effects of Ultrafine Particles. *Exp Mol Med*. 52 (3), 311–317. <https://doi.org/10.1038/s12276-020-0403-3>.
- Li, Y.; Lane, K. J.; Corlin, L.; Patton, A. P.; Durant, J. L.; Thanikachalam, M.; Woodin, M.; Wang, M.; Brugge, D., 2017. Association of Long-Term near-Highway Exposure to Ultrafine Particles with Cardiovascular Diseases, Diabetes and Hypertension. *Int J Environ Res*. 14 (5), 1–16. <https://doi.org/10.3390/ijerph14050461>.
- Chen, K.; Schneider, A.; Cyrys, J.; Wolf, K.; Meisinger, C.; Heier, M.; von Scheidt, W.; Kuch, B.; Pitz, M.; Peters, A.; Breitner, S., 2020. Hourly Exposure to Ultrafine Particle Metrics and the Onset of Myocardial Infarction in Augsburg, Germany. *Environ Health Perspect*. 128 (1), 1–10. <https://doi.org/10.1289/EHP5478>.
- HEI Review Panel on Ultrafine Particles, 2013. Understanding the Health Effects of Ambient Ultrafine Particles. HEI Perspectives 3. Health Effects Institute, Boston, MA. <https://www.healtheffects.org/system/files/Perspectives3.pdf>
- Brook, R. D.; Rajagopalan, S.; Pope, C. A.; Brook, J. R.; Bhatnagar, A.; Diez-Roux, A. v.; Holguin, F.; Hong, Y.; Luepker, R. v.; Mittleman, M. A.; Peters, A.; Siscovick, D.; Smith, S. C.; Whitsel, L.; Kaufman, J. D., 2010. Particulate Matter Air Pollution and Cardiovascular Disease: An Update to the Scientific Statement from the American Heart Association. *Circulation*. 121 (21), 2331–2378. <https://doi.org/10.1161/CIR.0b013e3181dbee1>.
- Du, Y.; Xu, X.; Chu, M.; Guo, Y.; Wang, J., 2016. Air Particulate Matter and Cardiovascular Disease: The Epidemiological, Biomedical and Clinical Evidence. *J Thorac Dis*. 8 (1), E8–E19. <https://doi.org/10.3978/j.issn.2072-1439.2015.11.37>.
- Andersen, Z. J.; Olsen, T. S.; Andersen, K. K.; Loft, S.; Ketzel, M.; Raaschou-Nielsen, O., 2010. Association between Short-Term Exposure to Ultrafine Particles and Hospital Admissions for Stroke in Copenhagen, Denmark. *Eur Heart J*. 31 (16), 2034–2040. <https://doi.org/10.1093/eurheartj/ehq188>.
- Downward, G. S.; van Nunen, E. J. H. M.; Kerckhoffs, J.; Vineis, P.; Brunekreef, B.; Boer, J. M. A.; Messier, K. P.; Roy, A.; Verschuren, W. M. M.; van der Schouw, Y. T.; Sluijs, I.; Gulliver, J.; Hoek, G.; Vermeulen, R., 2018. Long-Term Exposure to Ultrafine Particles and Incidence of Cardiovascular and Cerebrovascular Disease in a Prospective Study of a Dutch Cohort. *Environ Health Perspect*. 126 (12), 1–8. <https://doi.org/10.1289/EHP3047>.
- Centers for Disease Control and Prevention, 2018. Underlying Cause of Death, 1999-2018. CDC WONDER Online Database. <https://wonder.cdc.gov/>
- Aparicio, H. J.; Benjamin, E. J.; Callaway, C. W.; Carson, A. P.; Cheng, S.; Elkind, M. S. v.; Evenson, K. R.; Ferguson, J. F.; Knutson, K. L.; Lee, C. D.; Lewis, T. T.; Loop, M. S.; Lutsey, P. L.; Mackey, J.; Matchar, D. B., 2021. Heart Disease and Stroke Statistics-2021 Update: A Report from the American Heart Association. *Circulation*. 143, e254–e743. <https://doi.org/10.1161/CIR.0000000000000950>.
- Sioutas, C.; Delfino, R. J.; Singh, M., 2005. Exposure Assessment for Atmospheric Ultrafine Particles (UFPs) and Implications in Epidemiologic Research. *Environ Health Perspect*. 113 (8), 947–955. <https://doi.org/10.1289/ehp.7939>.

- Zhang, W.; Lin, S.; Hopke, P. K.; Thurston, S. W.; van Wijngaarden, E.; Croft, D.; Squizzato, S.; Masiol, M.; Rich, D. Q., 2018. Triggering of Cardiovascular Hospital Admissions by Fine Particle Concentrations in New York State: Before, during, and after Implementation of Multiple Environmental Policies and a Recession. *Environ Pollut.* 242, 1404–1416. <https://doi.org/10.1016/j.envpol.2018.08.030>.
- Rich, D. Q.; Zhang, W.; Lin, S.; Squizzato, S.; Thurston, S. W.; van Wijngaarden, E.; Croft, D.; Masiol, M.; Hopke, P. K., 2019. Triggering of Cardiovascular Hospital Admissions by Source Specific Fine Particle Concentrations in Urban Centers of New York State. *Environ Int.* 126 (October 2018), 387–394. <https://doi.org/10.1016/j.envint.2019.02.018>.
- Yu, F.; Luo, G., 2009. Simulation of Particle Size Distribution with a Global Aerosol Model: Contribution of Nucleation to Aerosol and CCN Number Concentrations. *Atmos Chem Phys.* 9 (20), 7691–7710. <https://doi.org/10.5194/acp-9-7691-2009>.
- Bey, I.; Jacob, D. J.; Yantosca, R. M.; Logan, J. A.; Field, B. D.; Fiore, A. M.; Li, Q.; Liu, H. Y.; Mickley, L. J.; Schultz, M. G., 2001. Global Modeling of Tropospheric Chemistry with Assimilated Meteorology: Model Description and Evaluation. *J Geophys Res Atmos.* 106 (D19), 23073–23095. <https://doi.org/10.1029/2001JD000807>.
- Luo, G.; Yu, F.; Moch, J. M., 2020. Further Improvement of Wet Process Treatments in GEOS-Chem V12.6.0: Impact on Global Distributions of Aerosols and Aerosol Precursors. *Geosci Model Dev.* 13 (6), 2879–2903. <https://doi.org/10.5194/gmd-13-2879-2020>.
- Holmes, C. D.; Bertram, T. H.; Confer, K. L.; Graham, K. A.; Ronan, A. C.; Wirks, C. K.; Shah, V., 2019. The Role of Clouds in the Tropospheric NO_x Cycle: A New Modeling Approach for Cloud Chemistry and Its Global Implications. *Geophys Res Lett.* 46 (9), 4980–4990. <https://doi.org/10.1029/2019GL081990>.
- Keller, C. A.; Long, M. S.; Yantosca, R. M.; da Silva, A. M.; Pawson, S.; Jacob, D. J., 2014. HEMCO v1.0: A Versatile, ESMF-Compliant Component for Calculating Emissions in Atmospheric Models. *Geosci Model Dev.* 7 (4), 1409–1417. <https://doi.org/10.5194/gmd-7-1409-2014>.
- Murray, L. T.; Jacob, D. J.; Logan, J. A.; Hudman, R. C.; Koshak, W. J., 2012. Optimized Regional and Interannual Variability of Lightning in a Global Chemical Transport Model Constrained by LIS/OTD Satellite Data. *J Geophys Res Atmos.* 117 (20), 1–14. <https://doi.org/10.1029/2012JD017934>.
- Pye, H. O. T.; Seinfeld, J. H., 2010. A Global Perspective on Aerosol from Low-Volatility Organic Compounds. *Atmos Chem Phys.* 10 (9), 4377–4401. <https://doi.org/10.5194/acp-10-4377-2010>.
- Evans, M. J.; Jacob, D. J., 2005. Impact of New Laboratory Studies of N₂O₅ Hydrolysis on Global Model Budgets of Tropospheric Nitrogen Oxides, Ozone, and OH. *Geophys Res Lett.* 32 (9), 1–4. <https://doi.org/10.1029/2005GL022469>.
- Martin, R. v.; Jacob, D. J.; Yantosca, R. M.; Chin, M.; Ginoux, P., 2003. Global and Regional Decreases in Tropospheric Oxidants from Photochemical Effects of Aerosols. *J Geophys Res Atmos.* 108 (3). <https://doi.org/10.1029/2002jd002622>.
- Yu, F.; Nadykto, A. B.; Herb, J.; Luo, G.; Nazarenko, K. M.; Uvarova, A. L. A., 2018. H₂SO₄-H₂O-NH₃ Ternary Ion-Mediated Nucleation (TIMN): Kinetic-Based Model and Comparison with CLOUD Measurements. *Atmos Chem Phys.* 18 (23), 17451–17474. <https://doi.org/10.5194/acp-18-17451-2018>.

581 Yu, F.; Luo, G.; Nadykto, A. B.; Herb, J., 2017. Impact of Temperature Dependence on the Possible
582 Contribution of Organics to New Particle Formation in the Atmosphere. *Atmos Chem Phys.* 17 (8), 4997–
583 5005. <https://doi.org/10.5194/acp-17-4997-2017>.
584
585 Yu, F., 2011. A Secondary Organic Aerosol Formation Model Considering Successive Oxidation Aging
586 and Kinetic Condensation of Organic Compounds: Global Scale Implications. *Atmos Chem Phys.* 11 (3),
587 1083–1099. <https://doi.org/10.5194/acp-11-1083-2011>.
588
589 Yu, F.; Luo, G.; Bates, T. S.; Anderson, B.; Clarke, A.; Kapustin, V.; Yantosca, R. M.; Wang, Y.; Wu, S.,
590 2010. Spatial Distributions of Particle Number Concentrations in the Global Troposphere: Simulations,
591 Observations, and Implications for Nucleation Mechanisms. *J Geophys Res Atmos.* 115 (17), 1–14.
592 <https://doi.org/10.1029/2009JD013473>.
593
594 Yu, F.; Luo, G.; Ma, X., 2012. Regional and Global Modeling of Aerosol Optical Properties with a Size,
595 Composition, and Mixing State Resolved Particle Microphysics Model. *Atmos Chem Phys.* 12 (13),
596 5719–5736. <https://doi.org/10.5194/acp-12-5719-2012>.
597
598 Yu, F.; Luo, G.; Pryor, S. C.; Pillai, P. R.; Lee, S. H.; Ortega, J.; Schwab, J. J.; Hallar, A. G.; Leaitch, W.
599 R.; Aneja, V. P.; Smith, J. N.; Walker, J. T.; Hogrefe, O.; Demerjian, K. L., 2015. Spring and Summer
600 Contrast in New Particle Formation over Nine Forest Areas in North America. *Atmos Chem Phys.* 15
601 (24), 13993–14003. <https://doi.org/10.5194/acp-15-13993-2015>.
602
603 Yu, F.; Luo, G.; Hallar, A. G., 2016. Vertical Profiles and Seasonal Variations of Key Parameters
604 Controlling Particle Formation and Growth at Storm Peak Laboratory. *Aerosol Air Qual Res.* 16 (3), 900–
605 908. <https://doi.org/10.4209/aaqr.2015.05.0368>.
606
607 Yu, F.; Nair, A. A.; Luo, G., 2018. Long-Term Trend of Gaseous Ammonia Over the United States:
608 Modeling and Comparison With Observations. *J Geophys Res Atmos.* 123 (15), 8315–8325.
609 <https://doi.org/10.1029/2018JD028412>.
610
611 Luo, G.; Yu, F., 2011. Sensitivity of Global Cloud Condensation Nuclei Concentrations to Primary
612 Sulfate Emission Parameterizations. *Atmos Chem Phys.* 11 (5), 1949–1959. <https://doi.org/10.5194/acp-11-1949-2011>.
613
614 Ma, X.; Yu, F.; Luo, G., 2012. Aerosol Direct Radiative Forcing Based on GEOS-Chem-APM and
615 Uncertainties. *Atmos Chem Phys.* 12 (12), 5563–5581. <https://doi.org/10.5194/acp-12-5563-2012>.
616
617 Ma, X.; Yu, F., 2014. Seasonal Variability of Aerosol Vertical Profiles over East US and West Europe:
618 GEOS-Chem/APM Simulation and Comparison with CALIPSO Observations. *Atmos Res.* 140–141, 28–
619 37. <https://doi.org/10.1016/j.atmosres.2014.01.001>.
620
621 Williamson, C. J.; Kupc, A.; Axisa, D.; Bilsback, K. R.; Bui, T. P.; Campuzano-Jost, P.; Dollner, M.;
622 Froyd, K. D.; Hodshire, A. L.; Jimenez, J. L.; Kodros, J. K.; Luo, G.; Murphy, D. M.; Nault, B. A.; Ray,
623 E. A.; Weinzierl, B.; Wilson, J. C.; Yu, F.; Yu, P.; Pierce, J. R.; Brock, C. A., 2019. A Large Source of
624 Cloud Condensation Nuclei from New Particle Formation in the Tropics. *Nature.* 574 (7778), 399–403.
625 <https://doi.org/10.1038/s41586-019-1638-9>.
626
627 Abrams, J. Y.; Weber, R. J.; Klein, M.; Sarnat, S. E.; Chang, H. H.; Strickland, M. J.; Verma, V.; Fang,
628 T.; Bates, J. T.; Mulholland, J. A.; Russell, A. G.; Tolbert, P. E., 2017. Erratum: Associations between
629 Ambient Fine Particulate Oxidative Potential and Cardiorespiratory Emergency Department Visits.
630 *Environ Health Perspect.* 125 (12), 129001. <https://doi.org/10.1289/EHP3048>.
631

632 Pieters, N.; Koppen, G.; van Poppel, M.; de Prins, S.; Cox, B.; Dons, E.; Nelen, V.; Panis, L. I.; Plusquin,
 633 M.; Schoeters, G.; Nawrot, T. S., 2015. Blood Pressure and Same-Day Exposure to Air Pollution at
 634 School: Associations with Nano-Sized to Coarse PM in Children. *Environ Health Perspect.* 123 (7), 737–
 635 742. <https://doi.org/10.1289/ehp.1408121>.
 636
 637 Olsen, Y.; Karottki, D. G.; Jensen, D. M.; Bekö, G.; Kjeldsen, B. U.; Clausen, G.; Hersoug, L. G.; Holst,
 638 G. J.; Wierzbicka, A.; Sigsgaard, T.; Linneberg, A.; Møller, P.; Loft, S., 2014. Vascular and Lung
 639 Function Related to Ultrafine and Fine Particles Exposure Assessed by Personal and Indoor Monitoring:
 640 A Cross-Sectional Study. *J Environ Health.* 13 (1), 1–10. <https://doi.org/10.1186/1476-069X-13-112>.
 641
 642 Breitner, S.; Peters, A.; Zareba, W.; Hampel, R.; Oakes, D.; Wiltshire, J.; Frampton, M. W.; Hopke, P. K.;
 643 Cyrus, J.; Utell, M. J.; Kane, C.; Schneider, A.; Rich, D. Q., 2019. Ambient and Controlled Exposures to
 644 Particulate Air Pollution and Acute Changes in Heart Rate Variability and Repolarization. *Sci Rep.* 9 (1),
 645 1–12. <https://doi.org/10.1038/s41598-019-38531-9>.
 646
 647 Rich, D. Q.; Zareba, W.; Beckett, W.; Hopke, P. K.; Oakes, D.; Frampton, M. W.; Bisognano, J.;
 648 Chalupa, D.; Bausch, J.; O'Shea, K.; Wang, Y.; Utell, M. J., 2012. Are Ambient Ultrafine, Accumulation
 649 Mode, and Fine Particles Associated with Adverse Cardiac Responses in Patients Undergoing Cardiac
 650 Rehabilitation? *Environ Health Perspect.* 120 (8), 1162–1169. <https://doi.org/10.1289/ehp.1104262>.
 651
 652 Peters, A.; Hampel, R.; Cyrus, J.; Breitner, S.; Geruschkat, U.; Kraus, U.; Zareba, W.; Schneider, A.,
 653 2015. Elevated Particle Number Concentrations Induce Immediate Changes in Heart Rate Variability: A
 654 Panel Study in Individuals with Impaired Glucose Metabolism or Diabetes. *Part Fibre Toxicol.* 12 (1), 1–
 655 11. <https://doi.org/10.1186/s12989-015-0083-7>.
 656
 657 Croft, D. P.; Cameron, S. J.; Morrell, C. N.; Lowenstein, C. J.; Ling, F.; Zareba, W.; Hopke, P. K.; Utell,
 658 M. J.; Thurston, S. W.; Thevenet-Morrison, K.; Evans, K. A.; Chalupa, D.; Rich, D. Q., 2017.
 659 Associations between Ambient Wood Smoke and Other Particulate Pollutants and Biomarkers of
 660 Systemic Inflammation, Coagulation and Thrombosis in Cardiac Patients. *Environ Res.* 154, 352–361.
 661 <https://doi.org/10.1016/j.envres.2017.01.027>.
 662
 663 Rückerl, R.; Schneider, A.; Hampel, R.; Breitner, S.; Cyrus, J.; Kraus, U.; Gu, J.; Soentgen, J.; Koenig,
 664 W.; Peters, A., 2016. Association of Novel Metrics of Particulate Matter with Vascular Markers of
 665 Inflammation and Coagulation in Susceptible Populations –Results from a Panel Study. *Environ Res.* 150,
 666 337–347. <https://doi.org/10.1016/J.ENVRES.2016.05.037>.
 667
 668 Hennig, F.; Quass, U.; Hellack, B.; Küpper, M.; Kuhlbusch, T. A. J.; Stafoggia, M.; Hoffmann, B., 2018.
 669 Ultrafine and Fine Particle Number and Surface Area Concentrations and Daily Cause-Specific Mortality
 670 in the Ruhr Area, Germany, 2009–2014. *Environ Health Perspect.* 126 (2), 2009–2014.
 671 <https://doi.org/10.1289/EHP2054>.
 672
 673 Sager, T. M.; Castranova, V., 2009. Surface Area of Particle Administered versus Mass in Determining
 674 the Pulmonary Toxicity of Ultrafine and Fine Carbon Black: Comparison to Ultrafine Titanium Dioxide.
 675 *Part Fibre Toxicol.* 6, 15. <https://doi.org/10.1186/1743-8977-6-15>.
 676
 677 Schmid, O.; Stoeger, T., 2017. Corrigendum to “Surface area is the biologically most effective dose
 678 metric for acute nanoparticle toxicity in the lung” [*Journal of Aerosol Science* 99 (2016) 133–143]. *J*
 679 *Aerosol Sci.* 113, 276. <https://doi.org/10.1016/j.jaerosci.2017.09.017>.
 680
 681 Hussain, S.; Boland, S.; Baeza-Squiban, A.; Hamel, R.; Thomassen, L. C. J.; Martens, J. A.; Billon-
 682 Galland, M. A.; Fleury-Feith, J.; Moisan, F.; Pairon, J. C.; Marano, F., 2009. Oxidative Stress and

Proinflammatory Effects of Carbon Black and Titanium Dioxide Nanoparticles: Role of Particle Surface Area and Internalized Amount. *Toxicology*. 260 (1–3), 142–149. <https://doi.org/10.1016/J.TOX.2009.04.001>.

Karotki, D. G.; Spilak, M.; Frederiksen, M.; Andersen, Z. J.; Madsen, A. M.; Ketznel, M.; Massling, A.; Gunnarsen, L.; Møller, P.; Loft, S., 2015. Indoor and Outdoor Exposure to Ultrafine, Fine and Microbiologically Derived Particulate Matter Related to Cardiovascular and Respiratory Effects in a Panel of Elderly Urban Citizens. *Int J Environ Res*. 12 (2), 1667–1686. <https://doi.org/10.3390/ijerph120201667>.

Schraufnagel, D. E.; Balmes, J. R.; Cowl, C. T.; de Matteis, S.; Jung, S.-H.; Mortimer, K.; Perez-Padilla, R.; Rice, M. B.; Riojas-Rodriguez, H.; Sood, A.; Thurston, G. D.; To, T.; Vanker, A.; Wuebbles, D. J., 2019. Air Pollution and Noncommunicable Diseases: A Review by the Forum of International Respiratory Societies' Environmental Committee, Part 1: The Damaging Effects of Air Pollution. *Chest*. 155 (2), 409–416. <https://doi.org/10.1016/j.chest.2018.10.042>.

Mathis, U.; Mohr, M.; Forss, A.-M., 2005. Comprehensive Particle Characterization of Modern Gasoline and Diesel Passenger Cars at Low Ambient Temperatures. *Atmos Environ*. 39 (1), 107–117. <https://doi.org/10.1016/j.atmosenv.2004.09.029>.

Kuhn, T.; Biswas, S.; Sioutas, C., 2005. Diurnal and Seasonal Characteristics of Particle Volatility and Chemical Composition in the Vicinity of a Light-Duty Vehicle Freeway. *Atmos Environ*. 39 (37), 7154–7166. <https://doi.org/10.1016/J.ATMOSENV.2005.08.025>.

Charron, A.; Harrison, R. M., 2003. Primary Particle Formation from Vehicle Emissions during Exhaust Dilution in the Roadside Atmosphere. *Atmos Environ*. 37 (29), 4109–4119. [https://doi.org/10.1016/S1352-2310\(03\)00510-7](https://doi.org/10.1016/S1352-2310(03)00510-7).

Herner, J.; Ying, Q.; Aw, J.; Gao, O.; Chang, D.; Kleeman, M., 2006. Dominant Mechanisms That Shape the Airborne Particle Size and Composition Distribution in Central California. *Aerosol Sci Technol*. 40 (10), 827–844. <https://doi.org/10.1080/02786820600728668>.

Herner, J. D.; Aw, J.; Gao, O.; Chang, D. P.; Kleeman, M. J., 2005. Copyright 2005 Air and Waste Management Association Size and Composition Distribution of Airborne Particulate Matter in Northern California: I—Particulate Mass, Carbon, and Water-Soluble Ions. *J Air Waste Manag Assoc*. 55 (1), 30–51. <https://doi.org/10.1080/10473289.2005.10464600>.

Li, N.; Georas, S.; Alexis, N.; Fritz, P.; Xia, T.; Williams, M. A.; Horner, E.; Nel, A., 2016. A Work Group Report on Ultrafine Particles (AAAAI) Why Ambient Ultrafine and Engineered Nanoparticles Should Receive Special Attention for Possible Adverse Health Outcomes in Humans. *J Allergy Clin Immunol*. 138 (2), 386–396. <https://doi.org/10.1016/j.jaci.2016.02.023.A>.

Hildebrandt, K.; Rückerl, R.; Koenig, W.; Schneider, A.; Pitz, M.; Heinrich, J.; Marder, V.; Frampton, M.; Oberdörster, G.; Wichmann, H. E.; Peters, A., 2009. Short-Term Effects of Air Pollution: A Panel Study of Blood Markers in Patients with Chronic Pulmonary Disease. Part Fibre Toxicol. 6, 25. <https://doi.org/10.1186/1743-8977-6-25>.

Möller, W.; Felten, K.; Sommerer, K.; Scheuch, G.; Meyer, G.; Meyer, P.; Häussinger, K.; Kreyling, W. G., 2008. Deposition, Retention, and Translocation of Ultrafine Particles from the Central Airways and Lung Periphery. *Am J Respir Crit Care Med*. 177 (4), 426–432. <https://doi.org/10.1164/rccm.200602->

733 301OC.

734

735 Oberdorster, G.; Ferin, J.; Lehnert, B. E., 1994. Correlation between Particle Size, in Vivo Particle
736 Persistence, and Lung Injury. *Environ. Health Perspect.* 102 (SUPPL. 5), 173–179.

737 <https://doi.org/10.1289/ehp.102-1567252>.

738